

See discussions, stats, and author profiles for this publication at: <https://www.researchgate.net/publication/267814029>

Toxicity, Bioaccumulation, and Biotransformation of Silver Nanoparticles in Marine Organisms

ARTICLE in ENVIRONMENTAL SCIENCE AND TECHNOLOGY · NOVEMBER 2014

Impact Factor: 5.33 · DOI: 10.1021/es502976y · Source: PubMed

CITATIONS

4

READS

204

9 AUTHORS, INCLUDING:



[Huanhua Wang](#)

Chinese Academy of Sciences

35 PUBLICATIONS 625 CITATIONS

SEE PROFILE



[Kirk G Scheckel](#)

United States Environmental Protection Agency

147 PUBLICATIONS 3,887 CITATIONS

SEE PROFILE



[Mark G Cantwell](#)

United States Environmental Protection Agency

66 PUBLICATIONS 1,122 CITATIONS

SEE PROFILE



[David R Katz](#)

United States Environmental Protection Agency

12 PUBLICATIONS 123 CITATIONS

SEE PROFILE

Toxicity, Bioaccumulation, and Biotransformation of Silver Nanoparticles in Marine Organisms

Huanhua Wang,^{†,‡} Kay T. Ho,^{*,†} Kirk G. Scheckel,[§] Fengchang Wu,^{*,‡} Mark G. Cantwell,[†] David R. Katz,[†] Doranne Borsay Horowitz,[†] Warren S. Boothman,[†] and Robert M. Burgess[†]

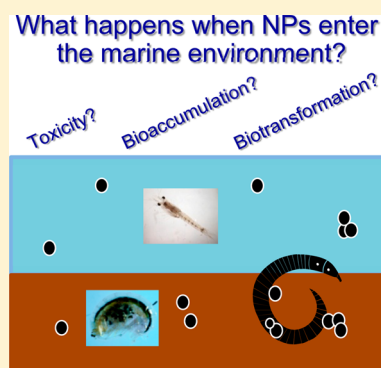
[†]U.S. Environmental Protection Agency, ORD/NHEERL/Atlantic Ecology Division, Narragansett, Rhode Island 02882, United States

[‡]State Key Laboratory of Environmental Criteria and Risk Assessment, Chinese Research Academy of Environmental Sciences, Beijing 100012, China

[§]U.S. Environmental Protection Agency, ORD/NRMRL/Land Remediation and Pollution Control Division, Cincinnati, Ohio 45224, United States

S Supporting Information

ABSTRACT: The toxicity, bioaccumulation, and biotransformation of citrate and polyvinylpyrrolidone (PVP) coated silver nanoparticles (NPs) (AgNP-citrate and AgNP-PVP) in marine organisms via marine sediment exposure was investigated. Results from 7-d sediment toxicity tests indicate that AgNP-citrate and AgNP-PVP did not exhibit toxicity to the amphipod (*Ampelisca abdita*) and mysid (*Americamysis bahia*) at ≤ 75 mg/kg dry wt. A 28-d bioaccumulation study showed that Ag was significantly accumulated in the marine polychaete *Nereis virens* (*N. virens*) in the AgNP-citrate, AgNP-PVP and a conventional salt (AgNO_3) treatments. Synchrotron X-ray absorption spectroscopy (XAS) results showed the distribution of Ag species in marine sediments amended with AgNP-citrate, AgNP-PVP, and AgNO_3 was AgCl (50–65%) > Ag_2S (32–42%) > Ag metal (Ag^0) (3–11%). In *N. virens*, AgCl (25–59%) and Ag_2S (10–31%) generally decreased and, Ag metal (32–44%) increased, relative to the sediments. The patterns of speciation in the worm were different depending upon the coating of the AgNP and both types of AgNPs were different than the AgNO_3 salt. These results show that the AgNP surface capping agents influenced Ag uptake, biotransformation, and/or excretion. To our knowledge, this is the first demonstration of the bioaccumulation and speciation of AgNPs in a marine organism (*N. virens*).



INTRODUCTION

Engineered nanoparticles (NPs) have recently been the focus of intense research because of their widespread and increasing usage and the potential risk they pose to human health and the environment. Silver nanoparticles (AgNPs) are commonly used in numerous consumer products including textiles, cosmetics, and health care items in order to exploit their strong antimicrobial activity.¹ The proliferation of applications and products containing NPs will inevitably result in the release of these materials into the environment, (e.g., atmosphere, surface/groundwater, soils/sediments, and marine environments). Currently, the ecotoxicological impacts of AgNPs in the marine environment are largely unknown.

Recent research has indicated AgNPs introduced into the marine environment will aggregate and precipitate into the sediments.^{2,3} Consequently, sediments and benthic organisms are expected to be the main sink and the ultimate receptor, respectively, for AgNPs in the marine environment.^{4,5} Therefore, spiking sediments with and studying the resultant dietary exposure of AgNPs is a relevant approach for investigation of the potential ecotoxicological impacts of AgNPs. The polychaete *Nereis virens* (*N. virens*) is an organism recom-

mended for sediment bioaccumulation tests and thus an appropriate choice for this study.⁶

Currently, the mechanisms for the biological uptake and distribution of NPs in marine organisms remain unclear. Two specific and related questions are (1) what are their effects when NPs are bioaccumulated by organisms and (2) will they be biotransformed into different chemical species. Regarding toxic effects, there is limited information on the bioaccumulation and toxicity of AgNPs to marine organisms. Further, in marine sediment contaminated with AgNPs, different chemical species such as AgCl , Ag_2S , and Ag^0 may be formed. Environmental transformations of AgNPs will strongly affect their surface properties and consequently their transport, reactivity, and bioavailability in sedimentary and biological systems. Although the physical properties of some nanoparticles such as uncoated cerium nanoparticles have been quantified in cell buffers and cell media,⁷ it remains unknown

Received: June 19, 2014

Revised: October 29, 2014

Accepted: November 4, 2014

Published: November 4, 2014

how the surface coatings of AgNPs (e.g., citrate, polyvinylpyrrolidone (PVP)) modulate the aggregation state and dissolution rates of the nanometallic core in sediments and marine organisms. However, these processes are proposed to be regulated by the surface charge and particle size of the NPs and the mechanisms of interaction of NPs in a biological system.^{8–11}

In this study, to address the two questions above, the acute toxicity of citrate and PVP coated AgNPs amended into sediments were determined using the marine amphipod (*Ampelisca abdita*) and mysid shrimp (*Americamysis bahia*). In addition, the bioaccumulation of the AgNPs and a conventional silver salt (AgNO₃) by the marine polychaete *N. virens* via sediment exposure over the course of 28 d was investigated. To characterize the uptake mechanisms and biotransformation of the AgNPs, synchrotron X-ray absorption spectroscopy was used. Synchrotron X-ray absorption spectroscopy (XAS) and micro-X-ray fluorescence imaging (XRF) can detect elemental species by comparing the shape of their spectra with those of reference materials (e.g., AgCl, Ag₂S, and Ag⁰) as well as map the distribution of metals. This novel application of these techniques provides reliable and convincing evidence for the speciation of metals in sediments and organisms and the transformation of AgNPs as they are transferred from the sediment to and into the organism.

MATERIALS AND METHODS

Characteristics of AgNPs. Thirty nm Biopure citrate coated and PVP coated AgNPs (AgNP-citrate and AgNP-PVP) were purchased from Nanocomposix Inc. (San Diego, CA, USA) at a concentration of 1000 mg/L. The material characteristics can be found at www.nanocomposix.com and SI Table S1. A conventional silver salt (AgNO₃) solution was dissolved in Milli-Q water at 1,079 mg Ag/L to represent dissolved Ag. A pure citrate solution was purchased as a background control. The hydrodynamic diameter and zeta potential of the AgNP-citrate and AgNP-PVP solutions are reported in Wang et al.⁴

Sediment Toxicity Test. Sediment toxicity tests were performed according to Ho et al.¹² Long Island Sound (LIS) control sediments were sieved through a 2 mm sieve and stored at 4 °C before use in the study. Amphipods were collected from the John H. Chafee National Wildlife Refuge at Pettaquamscutt Cove (Narrow River, Narragansett, RI, USA) (41°26.92' N, 71°27.51' W) in June 2010. This area is an estuarine wildlife refuge (salinity range is 20–30 ppt) of over 121 metric hectares of saltmarsh and surrounding forest habitat with no noted sources of contaminants. Organisms were brought to the laboratory and sieved to obtain young adults in the size range of 0.71 to 1.0 mm. Mysids were cultured in the laboratory, and 48-h-old organisms were used in the study. The 1000 mg/L AgNP-citrate and AgNP-PVP solutions were ultrasonicated for 1 h and then pipetted into LIS sediments to attain nominal concentrations of 0.75, 7.5, and 75 mg/kg dry sediment weight (DW). The amended sediments were mixed on a roller mill at 4 °C for 16 d. After the 16 d mixing period, for each toxicity test replicate, 20 g of amended or control sediments and 60 mL of filtered reconstituted 30 ppt salinity seawater were added to exposure chambers for each toxicity test replicate (*n* = 3). All exposure chambers were allowed to equilibrate for 24 h with gentle aeration prior to introducing ten amphipods and ten mysids to each chamber for the toxicity test. During the toxicity test (7 d), the amphipods were not fed; mysids were fed brine

shrimp *Artemia salina* *ad lib*. Dissolved oxygen and pH were measured on Day 5 with a Hach HQ30d (Loveland, Colorado, USA) and an Orion pH meter Model 230A (Boston, MA, USA), respectively. All exposure chambers were aerated, and the temperature was maintained at 22 °C ± 1 °C. At test termination, live and dead amphipods and mysids were counted, and the survival rates were calculated. Missing organisms were considered mortalities. At test termination, overlying seawater in the testing chambers was sampled, and the dissolved Ag was then measured by graphite furnace atomic absorption spectroscopy (GFAAS) (PerkinElmer, SIMAA 6000, MA, USA) with an analytical wavelength of 328.1 nm and a detection limit of approximately 0.5 µg/L.

Bioaccumulation Study. The bioaccumulation study was conducted according to U.S. EPA test methods.⁶ Sediments were amended using the same procedure as for the sediment toxicity test. The polychaetes *N. virens*, upon receipt from Aquatic Organism Research (NH, USA), were acclimated in clean LIS sediments with flow-through seawater for 5 d. The polychaetes were exposed for 28 d via a flow-through system to six treatments: a sediment control and sediments amended with 7.5 mg/kg DW of AgNP-citrate, AgNP-PVP, and AgNO₃. For each replicate, one *N. virens* was exposed to 200 mL wet sediments, and at least eight replicates were prepared for each treatment. The *N. virens* were not fed additionally during the exposure (i.e., they could process the sediments). Following exposure, samples of the sediment and *N. virens* were collected from each treatment. *N. virens* from five replicates were allowed to purge their gut contents by placing them in clean LIS for 1 d, while polychaetes from the other three replicates were not depurated and were immediately frozen. Of the five replicates of depurated polychaete samples, one was retained for synchrotron X-ray absorption spectroscopy (XAS) and micro-X-ray fluorescence imaging (XRF), while four were kept for total Ag measurement. The *N. virens* samples were rinsed with clean seawater and patted dry. *N. virens* and sediment samples were freeze-dried for 1 d and digested with concentrated nitric acid, and the Ag concentrations were measured by GFAAS.

Synchrotron X-ray Absorption Spectroscopy and Micro-X-ray Fluorescence Imaging. The synchrotron studies were conducted at the Advanced Photon Source, Argonne National Laboratory, (Argonne, IL, USA) in top-up mode at 7 GeV and a ring current of 101 mA. A 0.5 mm premonochromator slit width and a Si (111) double crystal monochromator detuned by 10% to reject higher-order harmonics was employed. Bulk XAS was conducted at the Sector 10 beamline, while micro-XAS (µ-XAS) and micro-X-ray fluorescence (µ-XRF) experiments were conducted at the Sector 20 beamline of the Advanced Photon Source. The monochromator beam energy position at both beamlines was calibrated by assigning the first inflection of the absorption K-edge of Ag metal foil to 25514 eV. The µ-XRF mapping energy was 26000 eV for Ag. Both the sediment and polychaete samples for synchrotron investigation were freeze-dried for 1 d, ground in an agate mortar and pestle under protection by liquid nitrogen, and then pressed into a pellet. The same tissue and sediment pellets were used for µ-XAS and µ-XRF imaging followed by bulk XAS analyses. The spatial distribution of Ag in the sediments and *N. virens* was measured by µ-XRF with a solid-state 13-element Ge detector (Canberra, Australia). Three or four XAS spectra for each bulk sample and µ-XRF points of interest were collected in fluorescence mode at room temperature. All spectra were placed on the same energy grid

and aligned to the Ag metal foil, averaged, and normalized, and the background was removed by spline fitting using the computer package-IFEFFIT.¹³

The internalized species of Ag were investigated by linear combination fitting (LCF). Accuracy of LCF results is dependent on the resolution capacity of the XAS data with a generally accepted error of $\pm 5\%$.¹⁴ AgCl, Ag₂S, and elemental Ag were used as reference materials for Ag as determined by principal component analysis (PCA). Other Ag reference materials considered included Ag-ligand complexes with humic acid, citrate, cystine, cysteine, and histidine; Ag sorbed to kaolin and ferrihydrite; and Ag oxide and carbonate. Spectra of the reference materials were collected in transmission mode at the sector 10 beamline. LCF was conducted on the normalized (E) XAS spectra of the standards and samples. The Levenberg–Marquardt least-squares algorithm was applied to a fit range of -20 to 80 eV. Best-fit scenarios were defined as having the smallest residual fitting error (χ^2), and the sum of all fractions was close to 1. To fully describe any particular sample within 1% reproducible error, a minimum of two components was necessary. LIS control sediment had very low levels of Ag, and the spectrum is not shown here as the concentration of Ag was too low to be detected by XAS.

Silver Extraction and Measurements. For sediment extractions of Ag, ~ 0.5 g of wet sediment from each treatment was weighed in 15 mL Teflon tubes (Saville, MN, USA), and then 9 mL of concentrated nitric acid (HNO₃) was added. The tubes were heated in a hot block (Digi PREP Jr, SCP Science, Quebec, Canada) at 95°C until ~ 1.0 mL acid remained in the tubes. Marine sediment reference materials MESS-3 and PACS-2 (Ottawa, Ontario, Canada) were used for quality control for the Ag extractions. The procedures for Ag extraction and measurements for *N. virens* were similar to those for sediments. To determine dissolved Ag in interstitial seawater, the sediments were centrifuged at 4000 g (IEC Centra-8R Centrifuge, USA) and passed through a $0.2\ \mu\text{m}$ PTFE syringe filter (Millipore Millex, Japan) and then dissolved Ag measured by GFAAS. Silver standard solutions ($1000\ \text{mg/L}$) purchased from Ultra Scientific Analytical Solutions (North Kingstown, RI, USA) were used for calibrations.

Statistical Analyses. Each treatment was performed in triplicate unless otherwise noted. Means and standard deviations are reported. Statistics analysis was performed using SPSS ver. 16.0 for Windows (SPSS, Chicago, IL, USA). One-way ANOVA (analysis of variance) with posthoc multiple comparisons (Tukey) was used to test for significant difference between treatments at the level of $p < 0.05$. Chi square (χ^2) values in XAS experiments are the statistical error estimates which provide a measure of the precision of the results and allow reasonable comparisons and is calculated as the ratio of the squared sums of $[\text{data-fit}]^2/[\text{data}]^2$.

RESULTS AND DISCUSSION

Sediment Toxicity Testing. During toxicity testing, overlying water pH ranged from 7.93 to 8.24, and dissolved oxygen was $8.1\text{--}8.9\ \text{mg/L}$ (greater than 90% saturation). Total Ag concentrations in the LIS sediment control and LIS sediment control amended with citrate solution were 0.62 and $0.51\ \text{mg/kg DW}$, respectively. Recovered total Ag concentrations in sediments from the AgNP-citrate, AgNP-PVP, and AgNO₃ treatments were significantly higher than the controls ($p < 0.05$ and $p < 0.01$) but not significantly different among the different treatments for the same amended concentration

(SI Figure S1). No toxicity was observed for either amphipods or mysids in the 7-d acute tests with any of the tested AgNPs or in the AgNO₃ treatments (SI Figure S2). The % survival of amphipods and mysids in the LIS control, AgNP-citrate, AgNP-PVP, and AgNO₃ treatments was 91.7 ± 7.5 , 93.3 ± 7.7 , 88.9 ± 7.3 , and 86.7 ± 4.4 , respectively.

The lack of toxicity is not entirely surprising in light of the equilibrium partitioning affecting the bioavailability of metals in sediments.^{15,16} The concentration of Ag added to the inorganic and NP treatments, $75\ \text{mg/kg}$, equals approximately $0.7\ \mu\text{mol/g}$, whereas LIS sediment typically contains $10\text{--}20\ \mu\text{mol}$ acid volatile sulfide (AVS)/g,^{17–19} greatly exceeding the $0.35\ \mu\text{mol/g}$ necessary to sequester the Ag as a solid phase sulfide and reduce interstitial water concentrations below a toxic threshold. Among others, Angel et al.² noted that adverse effects of silver were correlated to the ionic concentration of silver (Ag⁺). Background dissolved silver concentrations in seawater ranges from 0.15 to $2.9\ \mu\text{g/L}$ with an average of $0.29\ \mu\text{g/L}$.²⁰ The dissolved silver concentration in the overlying water of the testing chambers was 2.4 , 0.8 , and $4.1\ \mu\text{g/L}$ for $75\ \text{mg/kg DW}$ of AgNP-citrate, AgNP-PVP, and AgNO₃ treatments, respectively, and was not detected in the lower treatments. Berry et al.¹⁶ found a 10 d water only ionic Ag LC₅₀ of $20\ \mu\text{g Ag/L}$ for *A. abdita*, and Ward et al.⁵ reported 28-d *A. bahia* EC₂₀ values of 3.9 to $60\ \mu\text{g/L}$ at salinities of 10 , 20 , and 30 ppt.

The low concentrations of Ag measured in overlying seawater support the conjecture that dissolved silver reacts with chloride and sulfides in seawater to precipitate from solution as insoluble AgCl and Ag₂S. In addition, the tendency of AgNPs to increase in particle size and aggregate as salinity increases⁴ supports the lack of elevated Ag concentrations in overlying seawater and toxicity in this study.

Bioaccumulation Test. No mortality in *N. virens* was observed although tissue wet weight loss was observed for all treatments (SI Figure S3). Recovered Ag concentration (mg/kg DW) in sediments amended with $7.5\ \text{mg/kg DW}$ of AgNP-citrate, AgNP-PVP, and AgNO₃ after bioaccumulation study is given in SI Figure S4, and the % recoveries ranged between 83% and 115% . The total Ag concentrations (mg/kg DW) accumulated by *N. virens* in different treatments after the 28-d bioaccumulation study are shown in Figure 1. Compared to the control, *N. virens* in all of the Ag treatments had significantly increased Ag concentrations. Within any of the treatments, Ag concentrations were not statistically different between the nondepurated and depurated *N. virens*, largely due to the high variability among replicates; however, there appears to be a trend for depurated *N. virens* to have lower Ag concentrations than nondepurated worms. After depuration, the Ag concentration decreased by $\sim 45\%$ in the AgNP treatments and 11% in the AgNO₃ treatment. Also, Ag concentrations in the nondepurated *N. virens* were not significantly different among AgNP-citrate, AgNP-PVP, and AgNO₃ treatments. However, in the depurated treatments, Ag concentration in *N. virens* exposed to AgNO₃ was significantly higher than the AgNP-citrate and AgNP-PVP exposures ($p = 0.020$, $p = 0.030$, respectively). These results support a difference between AgNPs and ionic Ag (from AgNO₃) uptake or availability, the reason may be due to selective uptake or excretion. For example, the AgNP agglomerates inside *N. virens* are less mobile and may be easily excreted. This difference is also supported by other researchers^{11,21,22} and the synchrotron X-ray absorption spectroscopy data presented below.

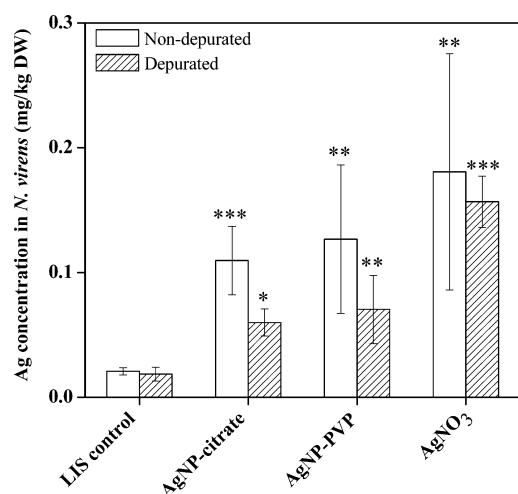


Figure 1. Ag concentrations (mg/kg DW) in *N. virens* in the Long Island Sound (LIS) control and the 7.5 mg/kg DW AgNP-citrate, AgNP-PVP, and AgNO₃ treatments after bioaccumulation for 28 d. Data are presented as the mean \pm standard deviation (SE) ($n = 3$ for nondepurated and $n = 4$ for depurated). Analysis of variance (ANOVA) was performed to identify differences between treatments. Compared to the control, *N. virens* in all of the Ag treatments had significantly increased Ag concentrations, *: $p < 0.1$, **: $p < 0.05$, ***: $p < 0.001$.

Synchrotron X-ray Absorption Spectroscopy (XAS) and Micro-X-ray Fluorescence (XRF) Imaging. The XAS data show the proportional distribution of Ag metal, AgCl, and Ag₂S species in the sediment and worms (Figures 2 and 3, SI Table S2). Figure 2 shows the XAS data (black curve) and LCF (red dots) for sediments and worms relative to Ag metal and AgCl and Ag₂S reference spectra data. Note the distinct structural features of the Ag metal and AgCl and Ag₂S reference spectra in visual comparison to the sample data in Figure 2 and corresponding LCF results in SI Table S2. The speciation of Ag

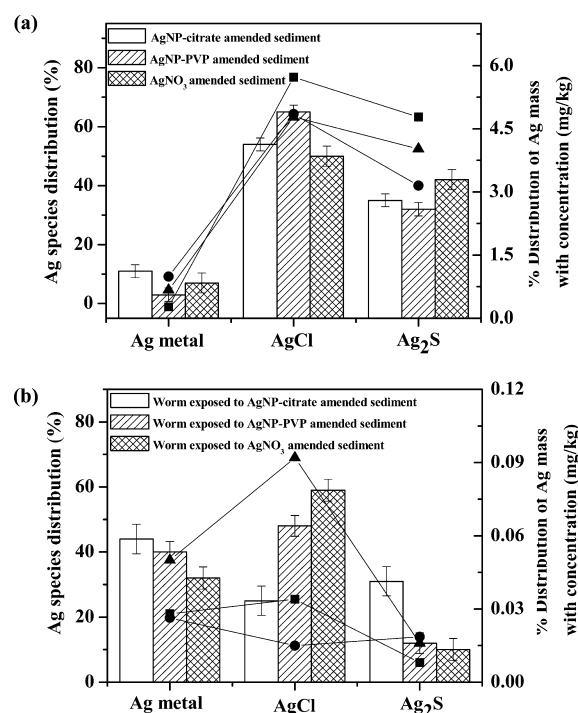


Figure 3. Bars show distribution (%) of Ag species (left Y-axis) in (a) sediments and (b) *N. virens* by form of Ag amended. The χ^2 values (in Table S2) $\times 100$ is the % error. The values graphed are the bulk XAS sediment and worm. a) Sediments - AgCl was the dominant overall species in sediments. b) *N. virens* - Ag metal distribution increased greatly in *N. virens* compared to the sediments. Speciation within *N. virens* varied by form of Ag to which *N. virens* was exposed. The lines represent the % distribution of Ag mass (right Y-axis) in (a) sediments and (b) *N. virens* with AgNP-citrate (●), AgNP-PVP (■), and AgNO₃ (▲) treatments.

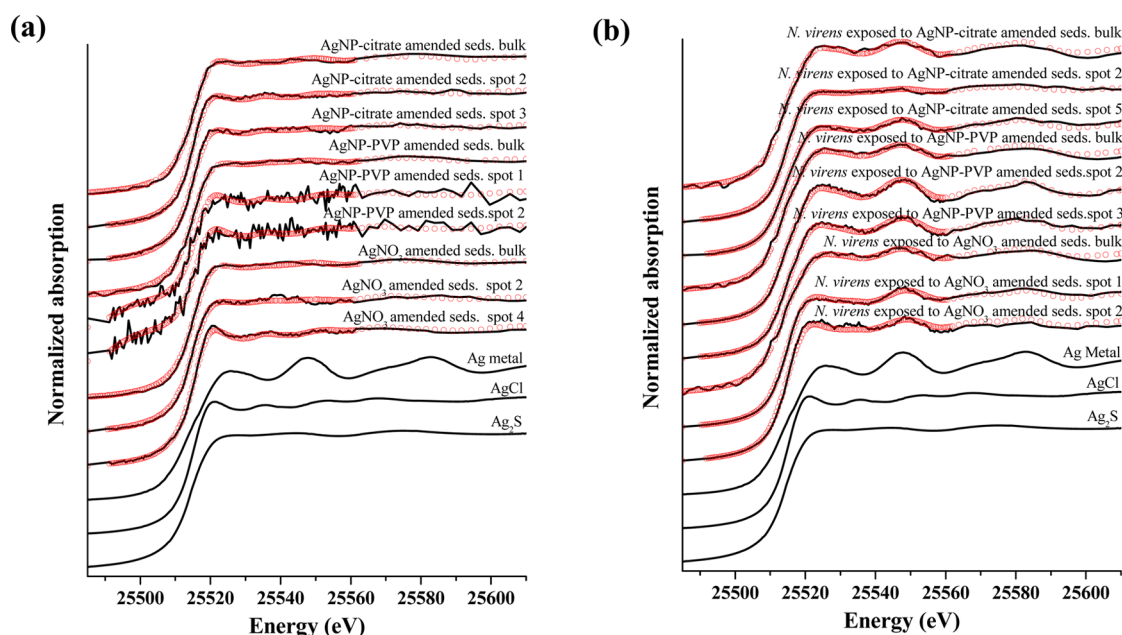


Figure 2. Synchrotron X-ray absorption spectroscopy (XAS) data of the (a) amended sediments (seds.) and (b) *N. virens* samples for the bulk and μ -XAS spots of interest and the reference materials Ag metal, AgCl, and Ag₂S. The black lines are the measured data, and the red circles are the linear combination fits.

in Ag metal was the same as that in AgNPs, (i.e., zero valence). The XAS bulk analysis integrated the Ag speciation signal over a 1 mm² area, while the spot data integrated a space of 3–4 μm². We chose to represent the bulk data, rather than the spot data (Figure 3a and b), as these numbers give a better overall picture of Ag speciation in sediments and worms. LCF results of bulk and spot data fitted against a variety of Ag species are presented in Table S2. The results showed that the distribution of Ag species in the sediments was mostly AgCl (50–65%), with some Ag₂S (32–42%) and little Ag metal (3–11%) (Figure 3a, SI Table S2), regardless of the form of Ag added. This observation supports predicted thermodynamic constraints of Ag speciation, which dictate that the majority of Ag would combine with chlorides in a chloride-rich environment such as seawater.²³

In the worms, the fractions of AgCl (25–59%) and Ag₂S (10–31%) decreased, and the fractions of Ag metal (32–44%) increased, relative to the sediments (Figure 3a and b, SI Table S2). Despite the apparent predominance of the AgCl form in the sediments, Ag speciation within the worm appears to depend on the original form of Ag to which the worms were exposed (Figure 3b). Worms exposed to AgNP-citrate had a relatively similar distribution among Ag metal, AgCl, and Ag₂S; whereas worms exposed to AgNP-PVP and AgNO₃ contained mostly Ag metal and AgCl. The AgCl fraction, which was the highest in the sediments, was lowest in the worms exposed to AgNP-citrate, followed by an increasing relative abundance for AgNP-PVP and AgNO₃, respectively. Additionally, the AgNP-citrate exposure had the highest Ag-metal fractions and the AgNO₃ exposure, the lowest Ag metal fraction. These patterns suggest the AgNP surface capping agents influence differential pathways of accumulation, biotransformation, and depuration in benthic organisms.

Reasons for the changing distributions of Ag species in *N. virens* with different Ag treatments, as well as between the sediment and *N. virens*, may include (1) chemical transformation of AgNPs, (2) *in vivo* bioreduction by *N. virens*, or (3) the preferential uptake or excretion of particular Ag species.

First, chemical transformation of AgNPs research suggests the formation of AgCl and Ag₂S are surface reactions creating a core–shell morphology, where the resulting NPs may retain a metallic core with a shell of oxidized reaction products.²³ Physical and chemical disruption of these core–shell NP aggregates within *N. virens* may result in relatively higher distributions of metallic Ag once the shell is disturbed and the metallic core is exposed. We hypothesize that the different coatings of these particles may have caused them to move along different kinetic pathways of transformation in the sediment, which may also account for the differences between the NP distributions in the worms. Differences in the speciation of Ag observed in the different treatments in the current study may be indicative of a continuum of transformation of the metal from the oxidized surface to the metallic Ag in the core. That is, as the aggregate of Ag metal core with a citrate/chloride surface is stripped to the metal core by a detoxifying step, the time frame may vary depending upon the surface shell coating. This hypothesis is supported by the energetics of citrate metabolism which is used by all aerobic organisms to generate energy.²⁴ Because citrate is a readily available source of energy for bacterial or enzymatic reactions within the worm, the citrate form AgNP would likely be the first to be metabolized leaving a metal core. This may account for the lower percentage of AgCl and the apparent higher percentage of Ag metal observed in the

AgNP-citrate treatment. In addition, worms from the AgNP-citrate treatment had a higher fraction of Ag₂S than did the AgNP-PVP and AgNO₃ treatments. Because PVP is not a preferred energy source compared to citrate,²⁵ the AgNP-PVP form would likely be stripped of its outside surface more slowly than citrate; and the AgNO₃ treatment, without any energy yielding capping compounds, would be the slowest to be metabolized. The above hypothesis is based on a one time snapshot of the metabolites and does not contain rate data; however, this order of metabolism and detoxification is the same order of Ag metal percentages seen in the XAS data (Figure 3, SI Table S2).

Second, *in vivo* bioreduction by *N. virens* is another possible explanation. Sintubin et al.²⁶ demonstrated the formation of AgNPs by *Lactobacillus* spp. from Ag solutions. Likewise, AgNPs were identified as resulting from *Bacillus subtilis* by reduction of Ag ions due to extracellular biosynthesis.²⁷ Marine polychaetes may isolate Ag metal in vacuoles, presumably as a detoxification mechanism.^{28,29} Ag from AgNPs was found associated with inorganic granules in estuarine polychaetes.²² In addition, to having a high Ag metal proportion, worms from the AgNP-citrate treatment had a higher fraction of Ag₂S than did the AgNP-PVP and AgNO₃ treatments. This may be a result of sulfur containing metallothionein proteins also used by the worm for detoxification^{22,28,29} or may reflect the worm's inability to break down the Ag₂S-citrate complex compared to Ag₂S-PVP or Ag₂S-Ag⁺ complexes.

Finally, the preferential uptake of AgNPs, may also occur, but in order for preferential uptake to be the predominant cause of the observed pattern of metal speciation, the worm would have had to preferentially uptake 4–17 times more Ag metal than AgCl and 4 to 37 times more Ag metal than Ag₂S (SI Table S3) based on the % mass distribution in the sediments compared to what is in the worms. While this may have occurred, we do not have an energetic reason to explain why worms would preferentially uptake such a larger amount of Ag metal relative to the other forms of Ag in the sediment which exist in greater proportions. In addition, the preferential excretion of certain forms of Ag may also play an important role in interpreting the % Ag distribution data. The increased presence of metallic Ag within *N. virens* (32–44%), even in the AgNO₃ treatment, suggests some biotransformation mechanism is active. These results indicate that Ag phases in the sediment were accumulated by *N. virens* and biotransformation of Ag took place internally and confirms, partially, the mechanisms given by Stark et al.¹¹

The synchrotron X-ray fluorescence (XRF) mapping detected concentrations of Ag in the sediments and *N. virens* samples (Figure 4). The controls were not analyzed by XRF as bulk analysis indicated they had very low levels of Ag. These qualitative XRF images provide some of the first direct evidence of AgNP uptake in *N. virens*. The images are pseudoquantitative in the sense that they are on the same intensity scale and of the same area size. The Ag spots in *N. virens* were less common than those in sediments and were irregularly distributed. Their locations were not correlated with sediment components such as Fe or Mn.

Environmental Implications. This study evaluated the toxicity and bioaccumulation of citrate and PVP coated AgNPs in a simplified marine system and provided important insight into the speciation and biotransformation of the two types of AgNPs. The AgNP-citrate, AgNP-PVP, and AgNO₃ treatments did not cause toxicity to the amphipods (*A. abdita*) and mysids

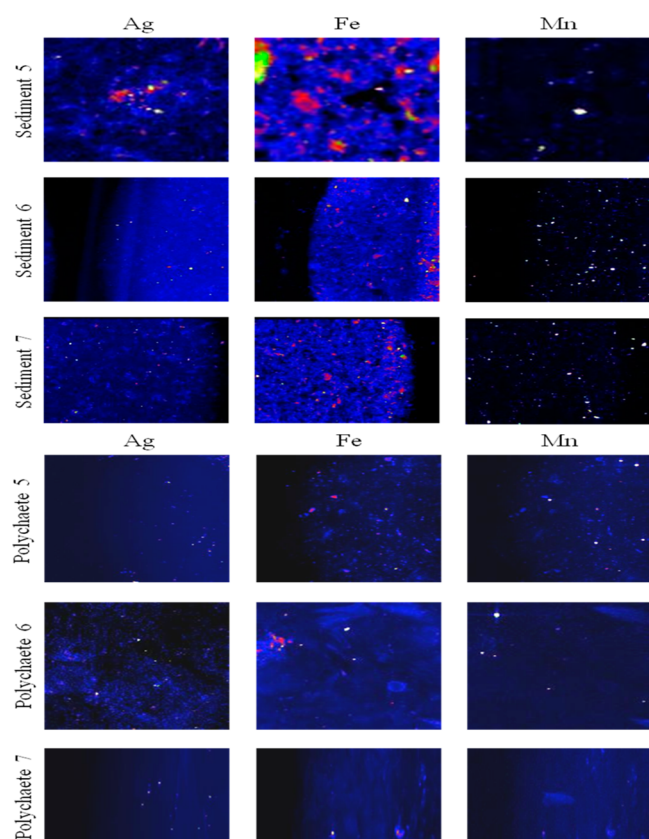


Figure 4. Synchrotron X-ray fluorescence (XRF) spectroscopy of the sediment and *N. virens* samples. Sediment samples “5”, “6”, and “7” were amended with 7.5 mg/kg DW of AgNP-citrate, AgNP-PVP, and AgNO₃, respectively. *N. virens* “5”, “6”, and “7” were exposed to the sediment “5”, “6”, and “7” for 28 d, respectively, and then depurated before the XRF measurement. Color intensity represents relative concentration from low (dark) to high (bright). Maps 5 and 6 are 1500 × 1500 μm; Map 7 is 1500 × 1000 μm.

(*A. bahia*) at concentrations up to 75 mg/kg DW. However, AgNPs were bioaccumulated by the marine polychaete (*N. virens*), and the accumulation order is AgNP-citrate < AgNP-PVP < AgNO₃. Synchrotron X-ray absorption spectroscopy showed that Ag metal and AgCl were the major *in vivo* forms in *N. virens*. In addition, in *N. virens* there were significant differences in Ag speciation distributions among AgNP-citrate, AgNP-PVP, and AgNO₃ treatments. Our results suggest that AgNP transformation rates are dependent on the capping agent with citrate being the most energetically favorable, followed by PVP and then ionic Ag. Mechanisms that support these observations include biotransformation, which is supported by the energetics observed in this experiment, but one cannot rule out selective uptake or excretion. Investigation of the speciation and biotransformation of NPs within exposed marine organisms is critical for understanding physiological, biochemical, and molecular modifications. Further, these modifications may also be important to understanding the potential risk of NPs through trophic transfer.³⁰ Overall, these results suggest that the risk assessment and regulation of AgNPs should consider the different bioaccumulation and biotransformation potential of AgNPs relative to ionic silver. Future studies could include Ag₂S and AgCl NPs to evaluate preferential uptake rates, development of more sensitive end points to determine *in*

in vivo effects of AgNPs, and understanding the mechanisms of the biotransformation of AgNPs in marine organisms.

■ ASSOCIATED CONTENT

Supporting Information

Additional 4 figures and 3 tables that contain data referenced in the main text. This material is available free of charge via the Internet at <http://pubs.acs.org>.

■ AUTHOR INFORMATION

Corresponding Authors

*K.T.H.: Fax: 401-782-3030. E-mail: ho.kay@epa.gov.

*F.W.: Fax: 86-10-84931804. E-mail: wufengchang@vip.skleg.cn.

Notes

The authors declare no competing financial interest.

■ ACKNOWLEDGMENTS

H. Wang was supported by the U.S. EPA as a National Research Council postdoctoral research associate. The authors wish to thank Drs. Todd Luxton, Walter Berry, and Shibin Li of the USEPA for their insightful reviews of this manuscript. This research used resources of the Advanced Photon Source, a U.S. Department of Energy (DOE) Office of Science User Facility operated for the DOE Office of Science by Argonne National Laboratory under Contract No. DE-AC02-06CH11357. Sector 20 facilities at the Advanced Photon Source, and research at these facilities, are supported by the US Department of Energy - Basic Energy Sciences, a Major Resources Support grant from NSERC, the University of Washington, the Canadian Light Source, and the Advanced Photon Source. Use of the Advanced Photon Source, an Office of Science User Facility operated for the U.S. Department of Energy Office of Science by Argonne National Laboratory, was supported by the U.S. DOE under Contract No. DE-AC02-06CH11357. The authors wish to thank Dr. Dale L. Brewe and Dr. Robert Gordon for assistance in X-ray absorption spectroscopy and X-ray fluorescence mapping at beamline 20-ID-B,C of PNC/XSD facilities. This research has been subject to U.S. EPA peer review; however, it does not necessarily reflect the views of the Agency. Mention of trade names of commercial products and companies does not constitute endorsement or recommendation for use. This is ORD # 007579.

■ REFERENCES

- (1) Wijnhoven, S. W. P.; Peijnenburg, W. J. G. M.; Herberets, C. A.; Hagens, W. I.; Oomen, A. G.; Heugens, E. H. W.; Roszek, B.; Bisschops, J.; Gosens, I.; Van de Meent, D.; Dekkers, S.; De Jong, W. H.; Van Zijverden, M.; Sips, A. J. A. M.; Geertsma, R. E. Nano-silver – a review of available data and knowledge gaps in human and environmental risk assessment. *Nanotoxicology* **2009**, 3 (2), 109–138.
- (2) Angel, B. M.; Batley, G. E.; Jarolimek, C. V.; Rogers, N. J. The impact of size on the fate and toxicity of nanoparticulate silver in aquatic systems. *Chemosphere* **2013**, 93, 359–365.
- (3) Klaine, S. J.; Alvarez, P. J.; Batley, G. E.; Fernandes, T. F.; Handy, R. D.; Lyon, D. Y.; Mahendra, S.; McLaughlin, M. J.; Lead, J. R. Nanomaterials in the environment: Behavior, fate, bioavailability, and effects. *Environ. Toxicol. Chem.* **2008**, 27 (9), 1825–1851.
- (4) Wang, H.; Burgess, R. M.; Cantwell, M. G.; Portis, L.; Perron, M. M.; Wu, F. C.; Ho, K. T. Stability and aggregation of silver and titanium dioxide nanoparticles in seawater: Role of salinity and dissolved organic carbon. *Environ. Toxicol. Chem.* **2014**, 33 (5), 1023–1029.

- (5) Ward, T. J.; Boeri, R. L.; Hogstrand, C.; Kramer, J. R.; Lussier, S. M.; Stubblefield, W. A.; Wyskiel, D. C.; Gorsuch, J. W. Influence of salinity and organic carbon on the chronic toxicity of silver to mysids (*Americamysis bahia*) and silversides (*Menidia beryllina*). *Environ. Toxicol. Chem.* **2006**, *25*, 1809–1816.
- (6) U.S. EPA/600/R-93/183, *Guidance manual: Bedded sediment bioaccumulation tests*; 1993.
- (7) Limbach, L. K.; Li, Y.; Grass, R. N.; Brunner, T. J.; Hintermann, M. A.; Muller, M.; Gunther, D.; Stark, W. J. Oxide nanoparticle uptake in human lung fibroblasts: Effects of particle size, agglomeration, and diffusion at low concentrations. *Environ. Sci. Technol.* **2005**, *39* (23), 9370–9376.
- (8) Sekine, R.; Khaksar, M.; Brunetti, G.; Donner, E.; Scheckel, K. G.; Lombi, E.; Vasilev, K. Surface immobilization of engineered nanomaterials for in-situ study of their environmental transformations and fate. *Environ. Sci. Technol.* **2013**, *47*, 9308–9316.
- (9) El Badawy, A. M.; Silva, R. G.; Morris, B.; Scheckel, K. G.; Suidan, M. T.; Tolaymat, T. M. Surface charge-dependent toxicity of silver nanoparticles. *Environ. Sci. Technol.* **2011**, *45* (1), 283–287.
- (10) El Badawy, A. M.; Scheckel, K. G.; Suidan, M.; Tolaymat, T. The impact of stabilization mechanism on the aggregation kinetics of silver nanoparticles. *Sci. Total Environ.* **2012**, *429*, 325–331.
- (11) Stark, W. J. Nanoparticles in biological systems. *Angew. Chem., Int. Ed.* **2011**, *50* (6), 1242–1258.
- (12) Ho, K. T.; Kuhn, A.; Pelletier, M.; Mc Gee, F.; Burgess, R. M.; Serbst, J. Sediment toxicity assessment: Comparison of standard and new testing designs. *Arch. Environ. Contam. Toxicol.* **2000**, *39*, 462–468.
- (13) Ravel, B.; Newville, M. ATHENA, ARTEMIS, HEPHAESTUS: Data analysis for X-ray absorption spectroscopy using IFEFFIT. *J. Synchrotron Radiat.* **2005**, *12*, 537–541.
- (14) Manceau, A.; Marcus, M. A.; Tamura, N. Quantitative speciation of heavy metals in soils and sediments by synchrotron X-ray techniques. In *Reviews in Mineralogy and Geochemistry, Applications of Synchrotron Radiation in Low-Temperature Geochemistry and Environmental Science*; Fenter, P., Rivers, M., Sturchio, N. C., Sutton, S., Eds.; Mineralogical Society of America: Washington, DC, 2002; Vol. 49, pp 341–428.
- (15) Burgess, R. M.; Berry, W. J.; Mount, D. R.; Di Toro, D. M. Mechanistic sediment quality guidelines based on contaminant bioavailability: Equilibrium partitioning sediment benchmarks. *Environ. Toxicol. Chem.* **2013**, *32* (1), 102–114.
- (16) Berry, W. J.; Cantwell, M. G.; Edwards, P. A.; Serbst, J. R.; Hansen, D. J. Predicting toxicity of sediments spiked with silver. *Environ. Toxicol. Chem.* **1999**, *18*, 40–48.
- (17) Ankley, G. T.; Phipps, G. L.; Leonard, E. N.; Benoit, D. A.; Mattson, V. R.; Kosian, P. A.; Cotter, A. M.; Dierkes, J. R.; Hansen, D. J.; Mahony, J. D. Acid-volatile sulfide as a factor mediating cadmium and nickel bioavailability in contaminated sediments. *Environ. Toxicol. Chem.* **1991**, *10*, 1299–1307.
- (18) Berry, W. J.; Hansen, D. J.; Boothman, W. S.; Mahony, J. D.; Robson, D. L.; Di Toro, D. M.; Shipley, B. P.; Rogers, B.; Corbin, J. M. Predicting the toxicity of metal-spiked laboratory sediments using acid-volatile sulfide and interstitial water normalizations. *Environ. Toxicol. Chem.* **1996**, *15* (12), 2067–2079.
- (19) Berry, W. J.; Boothman, W. S.; Serbst, J. R.; Edwards, P. A. Predicting the toxicity of chromium in sediments. *Environ. Toxicol. Chem.* **2004**, *23* (12), 2981–2992.
- (20) U.S. EPA Office of water regulations and standards criteria and standards division. *Ambient water quality criteria for silver*; 1980; p C-4.
- (21) Cong, Y.; Banta, G. T.; Selck, H.; Berhanu, D.; Valsami-Jones, E.; Forbes, V. E. Toxic effects and bioaccumulation of nano-, micron- and ionic Ag in the polychaete, *Nereis diversicolor*. *Aquat. Toxicol.* **2011**, *105*, 403–411.
- (22) García-Alonso, J.; Khan, F. R.; Misra, S. K.; Turmaine, M.; Smith, B. D.; Rainbow, P. S.; Luoma, S. N.; Valsami-Jones, E. Cellular internalization of AgNPs in gut epithelia of the estuarine polychaete, *Nereis diversicolor*. *Environ. Sci. Technol.* **2011**, *45*, 4630–4636.
- (23) Levard, C.; Hotze, E. M.; Lowry, G. V.; Brown, G. E., Jr. Environmental transformations of silver nanoparticles: Impact on stability and toxicity. *Environ. Sci. Technol.* **2012**, *46*, 6900–6914.
- (24) Stryer, L. *Biochemistry*, 2nd ed.; W.H. Freeman and Co.: San Francisco, CA, 1981.
- (25) Ravin, H. A.; Seligman, A. M.; Fine, J. Polyvinyl pyrrolidone as a plasma expander - Studies on its excretion, distribution and metabolism. *N. Engl. J. Med.* **1952**, *247*, 921–929.
- (26) Sintubin, L.; De Windt, W.; Dick, J.; Mast, J.; van der Ha, D.; Verstraete, W.; Boon, N. Lactic acid bacteria as reducing and capping agent for the fast and efficient production of silver nanoparticles. *Appl. Microbial. Biotechnol.* **2009**, *84* (4), 741–749.
- (27) Kannan, N.; Subbalaxmi, S. Green synthesis of silver nanoparticles using *Bacillus subtilis* IA751 and its antimicrobial activity. *Res. J. Nanosci. Nanotechnol.* **2011**, *1* (2), 87–94.
- (28) Koechlin, N.; Grasset, M. Silver contamination in the marine polychaete annelid *Sabella pavonina* S.: A cytological and analytical study. *Mar. Environ. Res.* **1988**, *26*, 249–263.
- (29) Vovelle, J.; Grasset, M. Experimental silver bioaccumulation in the polychaete *Pomatoceros triqueter* (L.): A cytological and micro-analytical study. *Biol. Met.* **1991**, *4*, 107–112.
- (30) Gardea-Torresdey, J. L.; Rico, C. M.; White, J. C. Trophic transfer, transformation, and impact of engineered nanomaterials in terrestrial environments. *Environ. Sci. Technol.* **2014**, *48*, 2526–2540.